DOI: 10.61782/fa.2023.0092

POINT TO POINT PROPAGATION OVER PERIODIC ROUGH BOUNDARIES

Keith Attenborough[1*] **Steve Mellish**[1] **Shahram Taherzadeh**[1]
Imran Bashir[2] **Alex Stronach**[3]
[1] School of Engineering and Innovation, The Open University, UK
[2] School of Computing, Engineering and Digital Technology, Teeside University, UK
[3] RPS Group, Manchester, UK

ABSTRACT

A rough surface formed by regularly spaced acoustically hard parallel strips or grooves gives rise to non-specular diffracted modes and surface waves. Surface waves result in values greater than +6 dB in spectra of the sound field relative to the direct field (excess attenuation). As well as surface wave generation, measurements of excess attenuation over regularly spaced parallel strips show effects of the finite array dimensions. Numerical predictions of pressure contours at the frequency of main surface wave energy show that the surface waves are created by overlapping, interacting, quarter wavelength resonances in the gaps between roughness elements or within grooves. Additional peaks in EA spectra result from interference between surface waves and diffracted components travelling towards the source. Surface waves are reduced if roughness elements resonate at surface wave frequencies. Predictions over periodic rectangular grooves with the same width but depths varied to create a phase change of 2π over each period show non-specular behaviour associated with surface wave generation and diversion of energy into diffracted modes. Useful traffic noise insertion loss due to a periodic surface consisting of rectangular grooves with different depths is predicted.

Keywords: *surface waves, periodic roughness, quarter wavelength resonance, excess attenuation.*

[*]***Corresponding author***: keith.attenborough@open.ac.uk.

1. INTRODUCTION

The solution for the sound field due to a point source in air over a rough acoustically hard boundary, for which the roughness height and spacing are small compared with the incident wavelength, includes an airborne surface wave which spreads cylindrically but attenuates exponentially both away from and along the surface [1]. Surface waves of this kind have been observed in laboratory experiments over rectangular grooves at ultrasonic frequencies [2], and, at audio-frequencies, over rectangular lattices [3,4], regularly spaced parallel cylinders [5], triangular wedges [6,7], and square and rectangular strips [7,8]. Outdoor measurements have indicated airborne surface waves over regularly spaced, parallel rows of bricks [9,10]. Surface waves can be detected in either frequency or time domains. Point-to-point propagation near a surface can be represented by the excess attenuation (EA) spectrum defined by,

$$EA = 20\log\left(\frac{p_{total}}{p_{direct}}\right) \quad (1)$$

Over an acoustically hard smooth surface the excess attenuation spectrum has a maximum of +6 dB which represents pressure doubling due to constructive interference between direct and ground-reflected sound pressure fields. Effectively, a rough hard boundary has a finite impedance and thereby causes a dip in the EA spectrum associated with destructive interference between the direct wave and the specular component of the reflected wave at a lower frequency than over a smooth hard surface. If a surface wave is generated, then the maximum exceeds +6 dB around the frequency of maximum surface wave energy. A roughness-induced surface wave appears in the time domain as a wave train following the direct and reflected wave component arrivals.

Surface waves over periodically-rough boundaries have been predicted numerically either by full discretization of the surface or via an effective impedance [11]. This paper reports measured EA spectra for regular and random strip arrangements, and measurements and predictions of finite array effects, the influences of quarter wavelength resonances and of resonant roughness elements. Also, a modal theory [12,13] is used to investigate traffic noise reduction through surface wave creation and the scattering of incident sound into non-specular diffracted modes by periodically grooved surfaces.

2. ARRAY SIZE AND BRAGG DIFFRACTION EFFECTS

Figure 1 compares anechoic laboratory measurements of EA spectra over surfaces composed of 15 parallel identical strips with triangular cross sections (base on a glass sheet either randomly or regularly spaced with (mean) centre-to-centre spacing of 0.05 m. The curve corresponding to random placement is the result of averaging EA spectra from five random distributions.

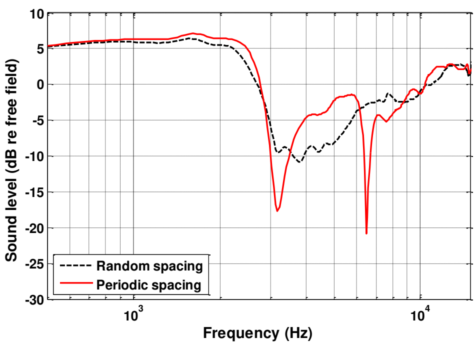

Figure 1. EA spectra measured with source and receiver at 0.07 m height separated by 0.7 m over an array of 15 triangular cross section strips on a glass sheet either regularly spaced (continuous line) or randomly distributed with a mean centre-to-centre spacing of 0.05 m (broken line) [10].

Regular spacing enhances the surface wave near 1.8 kHz and causes a narrowing and deepening of the first roughness-induced destructive interference between the direct and reflected waves which appears as a broad dip in the averaged EA spectrum for random arrangements. The first order Bragg diffraction at 3.5 kHz coincides with the first roughness induced EA dip. The 2nd order diffraction at 7 kHz is responsible for the second dip whereas the 2nd order roughness-induced EA dip for random arrangements is near 10 kHz and weaker.

Figure 2 shows the laboratory arrangement and Figure 3 compares measured EA spectra and Boundary Element Method (BEM) predictions with point source and receiver at heights of 0.05 m and 0.04 m respectively 0.7 m apart over an array of 30 parallel identical rectangular aluminium strips on a comparatively acoustically hard medium density fiberboard (MDF) without and with felt being placed along edges of the array parallel to the source-receiver axis [8].

Figure 2. Laboratory arrangement of an array of 30 × 1 m long parallel aluminium strips (height 0.025 m, width 0.0122 m) on MDF with felt along the array edges parallel to the source-receiver axis.

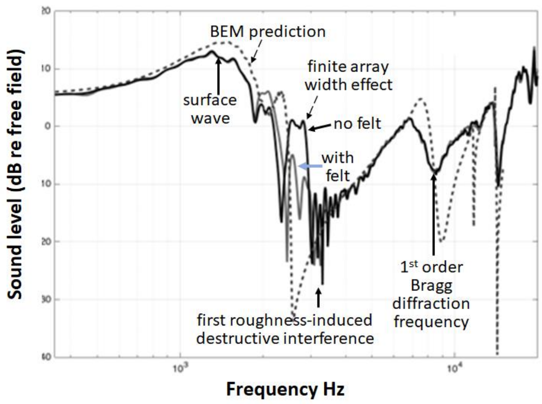

Figure 3. EA spectra measured with 0.05 m high source and 0.04 m high receiver separated by 0.7 m over an array of 30 identical parallel rectangular (0.025 m × 0.0122 m) strips with uniform edge to edge spacing of 0.015 m without and with felt along the edges parallel to the source-receiver axis on MDF. Also shown is a 2D BEM prediction (full discretization).

As well as the surface wave peak near 1.6 kHz, the peak near 2.5 kHz in the measured spectrum without the felt at the edges of the strip array is much reduced in the spectrum measured with felt present, indicating that it results from reflections at the ends of the strips. This effect is not predicted by a two-dimensional (2D) BEM used which assumes infinitely long strips.

If the gap width a between parallel rectangular strips of width w is sufficiently small, then the effective impedance of the array surface is that due to a hard-backed porous layer in which the pores are vertical slits (tortuosity = 1) and the porosity Ω and flow resistivity are given by [7,8,10]

$$\Omega = \frac{a}{a+w}, R_s = \frac{12\mu}{\Omega a^2}. \qquad (2)$$

Figure 4 compares EA spectra predicted using such a hard backed slit pore layer surface impedance and a BEM simulation for a fully discretized 2D array of 23 parallel identical rectangular (0.025 m × 0.0122 m) strips with edge to edge spacing of 0.0534 m. While both predictions show a surface wave at about 1.1 kHz, the BEM simulation shows additional peaks above this frequency, a deeper first minimum and extra minima at higher frequencies.

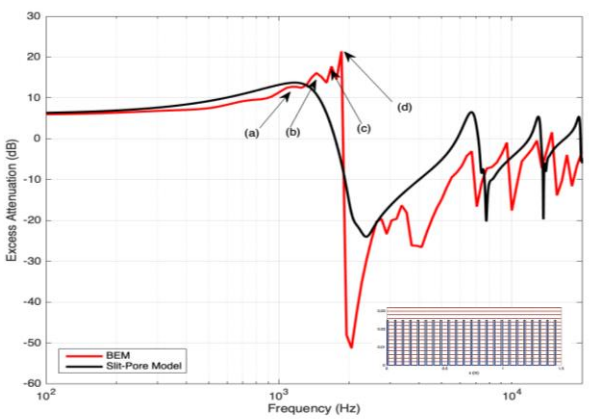

Figure 4. A comparison of EA spectra predicted by the slit pore model for 23 parallel identical rectangular strips separated by 0.0534 m (see inset) and predicted using a 2D BEM with full discretization.

Pressure contour plots obtained using a ContourBEM code developed at the Open University [8] at the frequencies corresponding to the arrows in Figure 4 are shown in Figure 5. At a frequency of 1.132 kHz, which corresponds to the lowest frequency peaks in the spectra predicted by both BEM calculations and the slit pore model, Fig. 6(a) shows a pattern of resonances within the gaps which can be considered to contribute to a surface wave. Stronger patterns of gap resonances are predicted at 1.45 kHz (Fig. 6(b)), 1.68 kHz (Fig.6(c)) and 1.86 kHz (Fig. 6(d)), which correspond to the second, third and fourth BEM-predicted peaks respectively. The 23-strip array length is 1.45 m and the standing wave pattern in Fig. 5(d) at 1.86 kHz is consistent with interference between a roughness-generated surface wave travelling at 273 m s^{-1} and a diffracted wave component travelling towards the source at a speed of 343 m s^{-1} [8]. The more complicated patterns in Fig.5 may involve interference with waves diffracted at angles other than grazing.

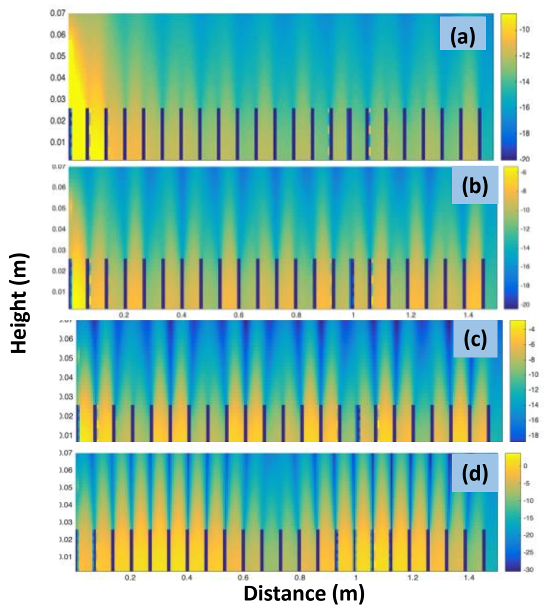

Figure 5. ContourBEM-predicted total pressure field over 23 periodically-spaced strips at (a) 1.132 kHz (b) 1.45 kHz, (c) 1.68 kHz, and (d) 1.86 kHz [8].

The influence of Helmholtz resonances on point-to-point propagation have been measured and predicted over hollow rectangular roughness elements with slits [14] and over a square array of tube-in-sphere resonators [15]. Figures 6 and 7 show measured EA spectra due to arrays of 20 × 0.5 m long PVC pipes with 0.04 m outer diameter (OD) without (Figure 6) and with (Figure 7) a single line of 0.00263 m wide 0.08 m long slots parallel to the axis. The slots cause a Helmholtz type of resonance in the cylinders and a corresponding dip in the EA spectrum at 680 Hz thereby reducing the roughness-induced surface wave contribution.

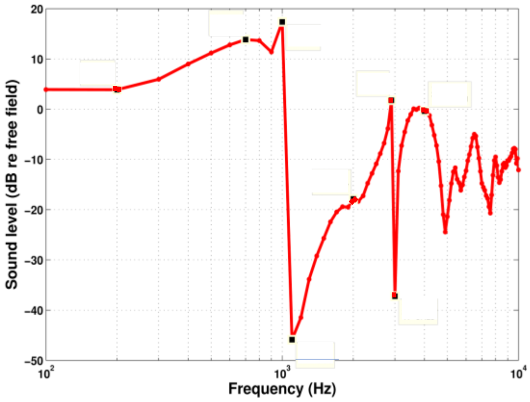

Figure 6. Measured EA spectra with 0.015 m high source and receiver separated by 2.0 m over MDF on which are placed arrays of 20 × 0.04 m OD PVC pipes centre-to-centre spacing of 0.1 m (no slots) [10].

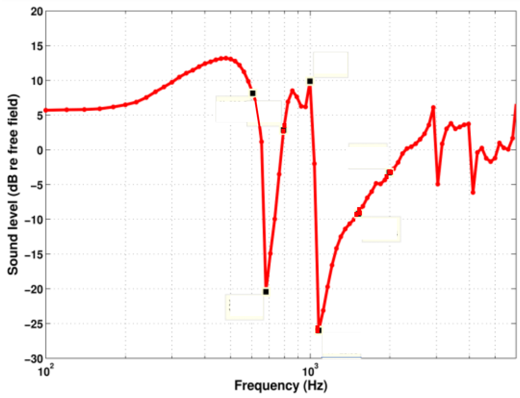

Figure 7. Measured EA spectra with 0.015 m high source and receiver separated by 2.0 m over MDF on which are placed arrays of 20 × 0.04 m OD PVC pipes with slots centre-to-centre spacing of 0.1 m [10].

Figure 8 (a) shows FEM-predicted total pressure contour plots, above the array of pipes without slots, at 700 Hz, which is near the roughness-generated surface wave peak, at 1 kHz. which corresponds to the peak resulting from the interference between surface and a backward propagating component, and at 1.1 kHz, which is the frequency of the dip in the EA spectrum caused by the first destructive interference associated with roughness-induced ground effect.

The pressure contour predictions in Fig. 8(b) above pipes with slots are at 600 Hz, which is slightly above the surface wave peak in the corresponding EA spectrum (Figure 7), at 700 Hz, just above the frequency of the slotted pipe Helmholtz resonance-induced EA dip and at 1 kHz, the frequency of the EA peak due to interference between the surface and a non-specular wave component travelling towards the source. Interaction between resonant roughness elements has been predicted for a surface consisting of adjacent identical slotted cylinders above an acoustically hard plane [16]. The pressure contour plots at 600 Hz and 1 kHz in Figure 8(b) show that the gap resonances and slotted pipe resonances merge and interact to strengthen and lower the frequency of the surface wave and cause an additional dip in the EA spectrum.

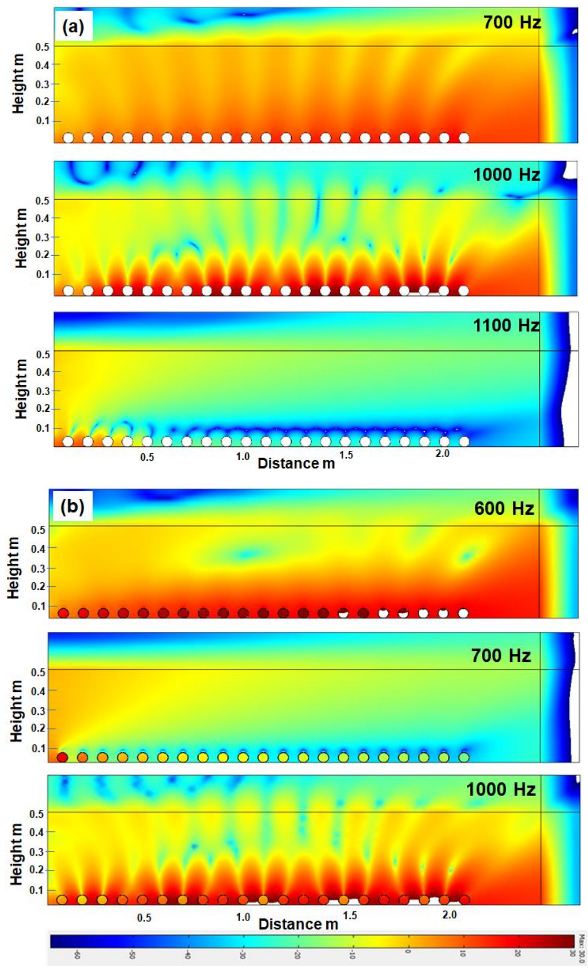

Figure 8. FEM (COMSOL®) predictions of total pressure field contours (a) at 0.7, 1 and 1.1 kHz over PVC pipes without slots and (b) at 0.6, 0.7 and 1 kHz over PVC pipes with slots.

3. QUARTER WAVE RESONANCES

The total pressure contour plots in Figures 5 and 8 show resonances in the gaps between strips and cylinders. Those in Figure 8(a) appear to merge to generate the surface wave. The impedance at the aperture to each gap dominates the effective impedance of a periodically rough surface. When the height of the gap is an odd multiple of one quarter of the incident wavelength ($\lambda/4$) the phase shift between downward and upward pressure components is π, so there is pressure cancelling at the aperture and significant energy is trapped in the gap. The $\lambda/4$ resonance phenomenon is modified by end effects at the apertures.

Using a modal model to predict the effective surface impedance, it is possible to show that, for parallel identical grooves, the frequencies of the minima in the spectrum of the magnitude of the effective impedance are related to the depth of the grooves and thereby, in turn, to the minima and maxima in the EA spectrum for point-to-point propagation across the grooves [17].

Interactions between quarter wave resonances in grooves are seen clearly in modal model predictions of point-to-point propagation over a periodically grooved surface where the period consists of two grooves with different depths (see Figure 9).

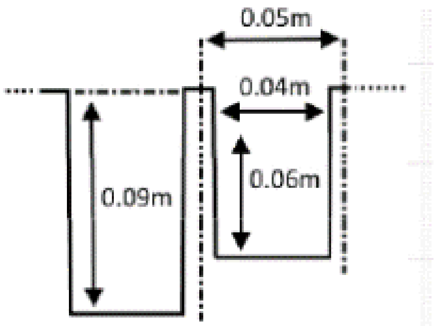

Figure 9. A two-groove period in a periodic surface with alternating groove depths.

The effective surface impedance for such a surface with d = 0.05 m, a = 0.04 m, h_0 = 0.086 m and h_1 = 0.057 m has been calculated using the modal model [12,20]. This effective impedance has been used to predict the EA spectrum shown in Figure 10 corresponding to source and receiver at 0.03 m height and separated by 2 m. The spectrum has peaks indicating surface waves at 700 Hz and 1030 Hz.

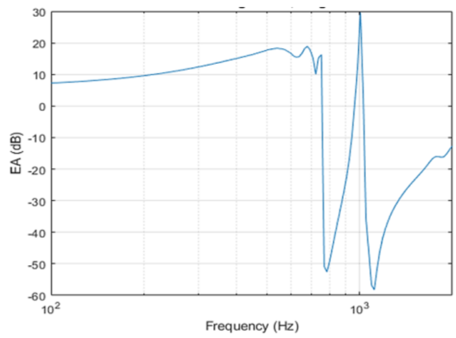

Figure 10. EA spectrum predicted for source and receiver at a height of 0.03 m and separated by 2 m over a periodically grooved surface with each two-groove period as shown in Figure 9 [20].

Figure 11 shows pressure contours calculated using BEM with full discretization of the periodically grooved surface, each period being composed of two grooves as shown in Figure 9. The upper plot is for a frequency of 752 Hz and the lower plot for 1006 Hz. These indicate that the EA spectrum peak at 752 Hz corresponds to a surface wave created by interacting resonances in the deeper grooves and the EA spectrum peak at 1006 Hz is associated with surface wave involving interacting resonances in the shallower grooves. Both plots show patterns associated with interference between the surface waves and backward propagating diffracted modes.

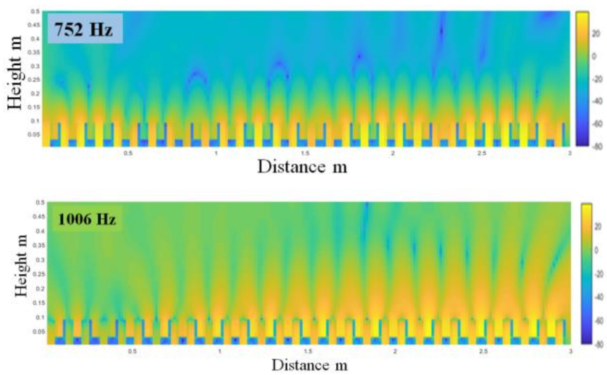

Figure 11. Pressure contours predicted by ContourBEM for 752 Hz and 1006 Hz corresponding to the surface wave peaks in the EA spectrum in Figure 10.

4. BLAZING

In Optics, the phenomenon by which incident energy is scattered or diffracted away from the specular reflection is known as blazing. It is possible to design optical gratings such that no energy is reflected in the specular direction [18]. Blazing by a periodically rough surface is aided by arranging for a phase change of 2 π over each period [19]. The modal model has been used to design a variable depth grooved surface to exploit this and give broadband excess attenuation near grazing incidence. Figure 12 shows a 5-groove period with depths between 0.03 m and 0.1 m.

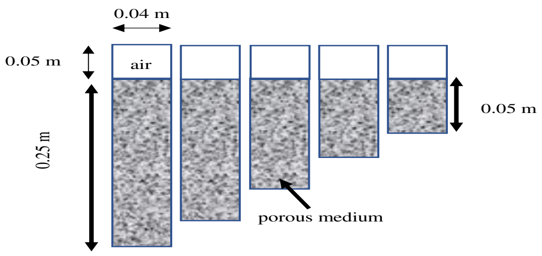

Figure 12. A five-groove period in a periodically grooved surface with varying depths and porous infill.

The slower sound speed in the porous infill (modelled as a slit pore medium with flow resistivity 1.74 kPa s m^{-2}) yields the target phase gradient with smaller depths and reduces the surface wave component. This design has been used, together with the effective impedance predicted by the modal model, to predict the influence on road traffic noise of a 5 m wide periodic variable depth groove assuming the arrangement shown in Figure 13. The source powers are calculated according to HARMONOISE [21].

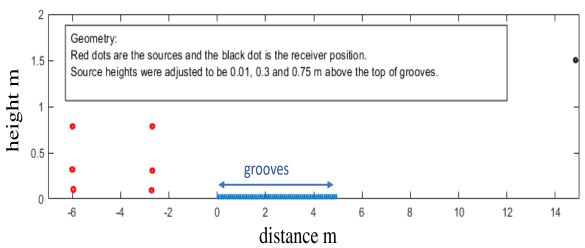

Figure 13. Schematic of assumed locations of road traffic sources, grooves and 1.5 m high receiver at 50 m from the nearest source.

In Figure 14 the predicted insertion loss (IL) spectrum for periodic variable depth grooved surface, with each period consisting of five grooves (see Figure 12), starting 1.5 m from the nearest assumed source locations is given by the broken line. That predicted with twice the groove depths but the same porous infill, is represented by the dotted line and shows an increase in IL below 300 Hz. The predicted IL spectrum for the Figure 12 design in which the porous infill has twice the original flow resistivity is given by the dash-dot line and shows a decrease in the influence of the surface wave.

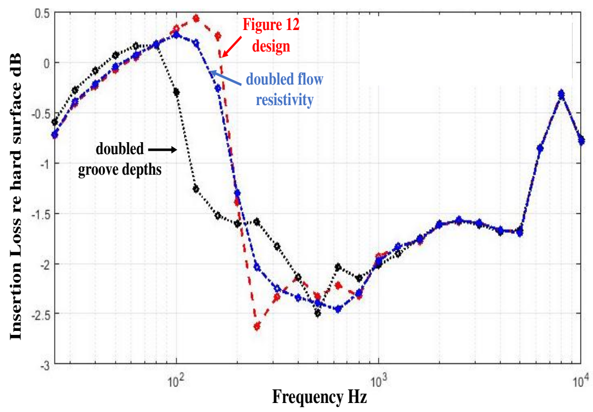

Figure 14. Modal Model Predictions of insertion loss spectra with respect to an acoustically hard smooth surface at a 1.5 m high receiver 50 m from an urban road due to a 5 m wide surface with 5-groove periods located 2.5 m from the nearest source (see Figure 13).

5. CONCLUDING REMARKS

Periodic rough surfaces, in which the roughness dimensions are small compared with the shortest wavelength of interest, give rise to surface waves of greater strength than randomly rough surfaces involving the same roughness heights and areal density. Several other aspects of point-to-point propagation over periodic rough surfaces have been investigated through laboratory measurements and numerical simulations. The finite size of the array results in extra peaks in the EA spectra. Quarter wavelength resonances interact in creating surface waves and there is interference between roughness-generated surface waves and diffracted waves travelling towards the source. Roughness element resonance can be used to reduce roughness-induced surface waves which otherwise would have adverse consequences, if using periodically rough surfaces for traffic noise reduction in situations where there is enough space and conventional noise barriers are not desirable. Non-specular reflection, assisted by creating a piecewise linear phase gradient of 2π over each period of the surface, reduces specular reflection and, thereby, improves the excess attenuation due to such surfaces.

6. ACKNOWLEDGMENTS

Parts of this work were supported by EPSRC UK grants EP/E063136/1 and EP/K03720X/1, COST Action 15125 DENORMS and EC FP7 Project number 234306 'HOSANNA'. AS was supported by a studentship funded by Komcept Systems Ltd, UK and the Open University.

7. REFERENCES

[1] I. Tolstoy: "Smoothed boundary conditions, coherent low-frequency scatter, and boundary modes," *J. Acoust. Soc. Am.* vol.75 pp. 1–22, 1984

[2] L. Kelders, J. Allard, and W. Lauriks: (1998). "Ultrasonic surface waves above rectangular groove gratings," *J. Acoust. Soc. Am.* vol. 103, pp. 2030–2033

[3] R. J. Donato, "Model experiments on surface waves", *J. Acoust. Soc. Am.* vol. 63, pp. 700–703, 1978.

[4] G. A. Daigle, M. R. Stinson and D. I. Havelock, "Experiments on surface waves over a model impedance plane using acoustical pulses," *J. Acoust. Soc. Am.* vol. 99**,** pp. 1993–2005, 1996.

[5] D. Berry, S. Taherzadeh and K. Attenborough, "Acoustic Surface Wave Generation over Rigid Cylinder Arrays on a Rigid Plane", *J. Acoust. Soc. Am.* vol. 146 pp. 2137–2144, 2019.

[6] H. Medwin, G. L. D. Spain, E. Childs and S. J. Hollis, "Low-frequency grazing propagation over periodic steep-sloped rigid roughness elements," *J. Acoust. Soc. Am.* vol. 76 pp. 1174–1190, 1984.

[7] I. Bashir, S. Taherzadeh, and K. Attenborough, "Surface waves over periodically-spaced strips" *J. Acoust. Soc. Am.* vol. 134, pp. 4691–4697, 2013.

[8] A. Stronach, *An investigation of the sound field above periodically spaced roughness*, PhD Thesis, Open University (2019)

[9] L. A. M. van der Heijden. and M. J. M. Martens, "Traffic noise reduction by means of surface wave exclusion above parallel grooves in the roadside", *Applied Acoustics* vol. 15 pp. 329–339, 1982.

[10] I. Bashir, *Acoustical exploitation of rough, mixed impedance and porous surfaces outdoors*, PhD Thesis, Open University (2014)

[11] K. Attenborough, and T. Van Renterghem, *Predicting Outdoor Sound 2nd edition*, CRC Press, Abingdon, UK, 2021.

[12] S. Mellish, S. Taherzadeh and K. Attenborough, "Approximate impedance models for point-to-point sound propagation over acoustically hard ground containing rectangular grooves", *J. Acoust. Soc. Am.* vol. 147, pp. 74–84, 2020.

[13] S. Mellish, S. Taherzadeh and K. Attenborough, "Use of a modal model in predicting the propagation of sound from a point source over a grooved surface", *Quart. J. Mech. Appl. Math*. Vol. 73 pp. 367–382, 2021.

[14] H-C Shin, S. Taherzadeh and K. Attenborough, "Ground effect due to periodic resonant roughness elements", *Proceedings of EuroNoise 2015*, Maastricht, The Netherlands (2015).

[15] K. Attenborough, H-C Shin, S. Taherzadeh *et al*, "Meta structures for Noise Control", *Proc. ICSV24*, London (2017)

[16] L. Schwan, O. Umnova and C. Boutin, "Effective behaviour of corrugated resonant surface emerging from near-field interactions" Proc. ICSV27, London (2017).

[17] S. Mellish, S. Taherzadeh and K. Attenborough, "Modal model prediction of surface waves and resonant characteristics of rectangular grooved gratings", *J. Acoust. Soc. Am.* Vol. 153 pp. 2932–2943 (2023)

[18] M. Memarian, X. Li, Y. Moromoto, and T. Itoh, "Wide band/angle blazed surfaces using multiple coupled blazing resonances", *Scientific Reports*, Vol.7 pp 42286 (2017).

[19] S. Larouche and D. Smith, "Reconciliation of generalized refraction with diffraction theory," *Optics Lett*. Vol 37 pp. 2391–2393.

[20] S. Mellish, S. Taherzadeh and K. Attenborough, “Audio-frequency surface waves over multiple InterNoise22, Glasgow (2022).

[21] HARMONOISE contract funded by the European Commission IST-2000-28419, https://cordis.europa.eu/project/id/IST-2000-28419 (last viewed 20/04/23), (2000)